Simulation of the Effect of Local Electric Potential and Substrate Concentration on CO_2 Reduction via Microbial Electrosynthesis

Vafa Ahmadi*, Carlos Dinamarca

Department of Process, Energy and Environmental Technology, University of Southeastern Norway
Vafa.Ahmadi@usn.no

Abstract

Integrating anaerobic digestion into electrochemical reactors is an advanced technology for biomethane recovery. Imposing low electric potential between electrodes, supplies CO_2, electrons, and hydronium ions from anodic oxidation of organic and/or inorganic compounds. Then, autotrophic methanogens on the cathode produce methane from CO_2 and H^+ by electron uptake from the cathode. However, in mixed microbial environments, acetogens produce acetate as well. These reactions can take place via two different mechanisms, DIET (direct interspecies electron transfer) or IMET (indirect mediated electron transfer). This work investigates CO_2 conversion to acetate and methane in an electrochemical biofilm reactor comparing the efficiency of CO_2 reduction via DIET and IMET mechanisms at hydrogen evolving potentials from -0.3 to -0.7 vs SHE. The other goal is to prove the importance of mass balance in CO_2 reduction at applied voltages. Simulations are done in AQUASIM version 2.1. Simulation results depicted that higher H^+ concentration at -0.7 V vs SHE can reduce more CO_2 in DIET with less current generation compared to IMET. This shows DIET the more efficient mechanism. Methane production is dominant in IMET model, however higher current is needed for CO_2 fixation in this mechanism. Also, biomass concentration, acetate and methane production, substrate concentration, biofilm thickness, biomass distribution in biofilm, and current density over time in both mechanisms are investigated at variant voltages and substrate concentrations. Simulations showed that at high CO_2 levels in both mechanisms CO_2 conversion cannot reach maximum if the voltage is not high enough to supply H^+.

Keywords: biofilm reactor, cathode, DIET, IMET, CO_2 conversion, methane, acetate

1. Introduction

Microbial electrosynthesis systems (MES) can solve the limitations of anaerobic digestion which have gained attention as power to gas technology; PtG in recent years (Nelabhotla et al., 2021). Biogas normally contains 50-70% CH_4, 50-30% CO_2 and other trace elements. Microbial communities can be stimulated to higher biogas production by a slight increase in the redox potential of the microbial environment. Applying low electric potentials between electrodes to execute electron transfer from anodic to cathodic biofilm has several advantages. Low voltage in the range of microbial redox activities triggers microorganisms to produce more biogas for a longer period and convert more CO_2 to methane. likewise, CH_4 content in biogas reaches up to 90-98%. This could happen when autotrophic microbes namely methanogens and mediator-producing microbes as acetogens contribute to CO_2 reduction via consumption of the available hydrogen. In these systems, CO_2 and hydrogen could be products of anodic dissociation of organic compounds such as complex carbohydrates or inorganic substances such as ammonium (Nelabhotla & Dinamarca, 2018; Sivalingam et al., 2020). Autotrophic methanogenesis and acetogenesis (equations 1 to 3) could take place via indirect mediated electron transfer (IMET)[1]:

$$2H^+ + 2e^- \rightarrow H_2\,, \qquad \Delta E^\circ = -0.414\,V \quad (1)$$

$$CO_2 + 4H_2 \rightarrow CH_4 + 2H_2O, \qquad \Delta G^0 = -16.35\,{}^{kJ}/_{e.eq} \quad (2)$$

$$2CO_2 + 4H_2 \rightarrow CH_3COO^- + 2H_2O, \Delta G^0 = -12.78\,{}^{kJ}/_{e.eq} \quad (3)$$

Or via equations 4 and 5 corresponding to direct interspecies electron transfer (DIET) (Nelabhotla & Dinamarca, 2019):

$$CO_2 + 8H^+ + 8e^- \rightarrow CH_4 + 2H_2O, \qquad \Delta E^0 = -0.248\,V \quad (4)$$

$$2CO_2 + 8H^+ + 8e^- \rightarrow CH_3COO^- + 2H_2O, \quad \Delta E^0 = -0.28V \quad (5)$$

In a microbial electrosynthesis system, both mechanisms are possible depending on the microbial species types. According to equation 1, IMET needs higher applied potentials to happen

[1] Voltage values in the paper are stated versus standard hydrogen electrode (vs, SHE)

compared to DIET. This makes IMET less energy efficient since higher potentials are necessary to supply electrons and H^+ for H_2 formation. However, if the inflow to the MES reactor is fully digested, it has low volatile fatty acids (VFAs), but high amounts of hardly degradable organic compounds and soluble CO_2. Such systems are dependent on hydrogen evolving potentials to provide H^+ for CO_2 fixation. It is important the potentials must be lower than the voltage required for water electrolysis in single chamber MES to avoid oxygen formation that is toxic for anaerobes. Electroactive hydrogen producing bacteria can produce hydrogen via IMET (Gharbi, et al., 2022). Hydrogenotrophic methanogens are of this kind which can produce hydrogen and consume it again for CO_2 fixation to methane (Berghuis et al., 2019). Tremblay et al. (Tremblay et al., 2019), reported that in an enriched medium with microbiome *S. Ovata* known as a hydrogen producing species, a gradual increase in the cathodic voltage from -0.3 to -0.7 vs, SHE, increased microbial H_2 evolution in the MES system. In another work, acetate production happened parallel to methane and hydrogen gas formation in a mixed microbial broth of chemolitoautotrophs at -0.9 V vs SHE on cathode (Bajracharya et al., 2015). Although theoretical reactions in equations 1 to 5 show a lower voltage, the local potential reported for hydrogen gas evolution, acetate and CH_4 formation is higher than the theoretical values. The reason is to overcome potential losses in the MES reactor which depend on factors such as the feed, microbial medium, electrode material, electrode surface area and the reactor volume. This study simulates autotrophic CO_2 conversion to CH_4 and acetate via DIET and IMET mechanisms which depend highly on the microbial community in the reactor. Not much particular work is available to compare DIET and IMET mechanisms. Nevertheless, in a modelling performed by Storck et al, DIET is suggested more advantageous for microbes because of fewer thermodynamic barriers (Storck et al., 2016). It is difficult to control microbial communities, however if the more efficient mechaism is found, the process operation can be controlled to increase the microbial species that demand less energy for CO_2 capture i.e, lower electron flow requirement for the process.

2. Methodology

The simulation is based on a single chamber biofilm reactor. Anode and cathode are in the same microbial medium. The reactor is fully mixed and has continuous inflow and discharge. Figure 1 shows the scheme of the model.

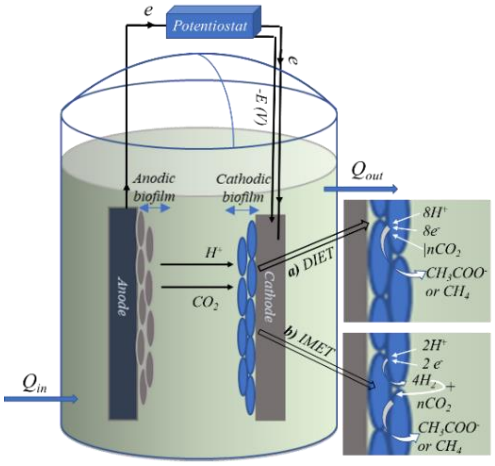

Figure 1. A schematic overview of a single chamber anaerobic MES reactor. The external electric potential on the cathode leads to bio anodic oxidation of organic or inorganic components and generation of CO_2/H^+ that transfer in the liquid toward the cathodic biofilm, and electrons which flow through the wire connection from anode to cathode. Cathodic biofilm ingests the substrates together with electrons to produce acetate (n=2) or methane (n=1) via two possible mechanisms: a) DIET or b) IMET.

2.1. Model assumptions and expressions

Assumptions of the model are as follows:

- The reactor operates at 1 atm and pH 7.
- Physiochemical gas/liquid mass transfer is not included. Diffusion and convection are assumed between liquid and biofilm.
- Effect of electrode material is not incorporated.
- Only cathodic reactions and cathodic biofilm is included in the simulated model.
- The source of H^+ for cathode is limited. H^+ values in the simulation are taken from experimental work based on anodic oxidation of organic compounds corresponding to a certain applied potential. However, anodic reactions are not included in the simulations.
- CO_2 is the carbon source for cathode which is soluble and in equilibrium with HCO_3^-.
- The active biomass is attached to cathode. Collaboration of the detached biofilm and suspended media to redox reactions is ignored.
- Initial biomass fraction is equal for all species. In DIET model, biomass consists of acetogens and methanogens. In IMET model, hydrogenotrophs are added to the other two species.
- The detachment velocity in the simulation (Reichert, 1998) is assumed as an indicator of bacterial decay (K_d) and loss of biofilm due to operating conditions.

In IMET model, hydrogenotrophic microbes produce hydrogen molecule at cathode. So, the electron acceptor in Monod expression is H^+ ion. Cathode performs as electron donor in the Nernst

term (equation 6). Autotrophic methanogens and acetogens take part in H_2 consumption (equations 7 and 8) which is expressed by multiplicative Monod equation. Cathodic reactions are the opposite of anode. therefore, the Nernst term is positive to represent cathode where electrons are taken from cathode and the voltage is negative (Flowers & Theopold, 2019; Metcalf et al., 2014; Torres et al., 2007).

$$\frac{d[X_{H_2}]}{dt} = X_{H_2} \cdot \left(\mu_{X_{H_2}}^{max} \cdot \frac{S_{H^+}}{K_{H^+}+S_{H^+}} \cdot \frac{1}{1+exp\left[(E_{app})\frac{2F}{RT}\right]} - k_{d,H_2}\right) \quad (6)$$

$$\frac{d[X_{CH_4}]}{dt} = X_{CH_4} \cdot \left(\mu_{X_{CH_4}}^{max} \cdot \frac{S_{CO_2}}{K_{CO_2}+S_{CO_2}} \cdot \frac{S_{H_2}}{K_{H^+}+S_{H^+}} - k_{d,CH_4}\right) \quad (7)$$

$$\frac{d[X_{ac}]}{dt} = X_{ac} \cdot \left(\mu_{X_{ac}}^{max} \cdot \frac{S_{CO_2}}{K_{CO_2}+S_{CO_2}} \cdot \frac{S_{H_2}}{K_{H_2}+S_{H_2}} - k_{d,ac}\right) \quad (8)$$

In DIET, microbes take electrons directly from cathode and consume H^+ and CO_2 from the bulk liquid. H^+ and CO_2 are both the limiting electron acceptor substrates. Therefore, Nernst-Monod equations in DIET can be expressed as in equations 9 and 10.

Product concentration in IMET and DIET is calculated according to equations 11 and 12.

$$\frac{d[X_{CH_4}]}{dt} = X_{CH_4} \cdot \left(\mu_{X_{CH_4}}^{max} \cdot \frac{1}{1+exp\left[(E_{app})\frac{8F}{RT}\right]} \cdot \frac{S_{CO_2}}{K_{CO_2}+S_{CO_2}} \cdot \frac{S_{H^+}}{K_{H^+}+S_{H^+}} - k_{d,CH_4}\right) \quad (9)$$

$$\frac{d[X_{AC}]}{dt} = X_{AC} \cdot \left(\mu_{X_{AC}}^{max} \cdot \frac{1}{1+exp\left[(E_{app})\frac{8F}{RT}\right]} \cdot \frac{S_{CO_2}}{K_{CO_2,HCO_3^-}+S_{CO_2}} \cdot \frac{S_{H^+}}{K_{H^+}+S_{H^+}} - k_{d,ac}\right) \quad (10)$$

$$\frac{d[S_{CH_4}]}{dt} = \left(\frac{d[X_{CH_4}]}{dt}\right) / Y_{CH_4} \quad (11)$$

$$\frac{d[S_{ac}]}{dt} = \left(\frac{d[X_{ac}]}{dt}\right) / Y_{ac} \quad (12)$$

Change in j (current density, $A \cdot m^{-2}$) over time correlates to electroactive biomass concentration, obtained by equation 13 (Torres et al., 2008).

$$\frac{dj}{dt} = \frac{d[X_i]}{dt} \cdot \gamma \cdot L_f \cdot (f_s^0 - 1) \quad (13)$$

Table 1. Model parameters for the simulation

Parameter	Symbol	Value	Unit	Ref
Specific respiration rate of microorganisms	b_X	0.05	d^{-1}	[a]
Diffusivity of acetate	D_{ac}	$1.54 \cdot 10^{-5}$	$m^2 \cdot d^{-1}$	[b]
Diffusivity of methane	D_{CH_4}	$1.296 \cdot 10^{-4}$	$m^2 \cdot d^{-1}$	[b]
Diffusivity of CO_2	D_{CO_2}	$1.658 \cdot 10^{-4}$	$m^2 \cdot d^{-1}$	[b]
Diffusivity of H_2	D_{H_2}	$3.88 \cdot 10^{-5}$	$m^2 \cdot d^{-1}$	[b]
Diffusivity of hydrogen ion (H^+)	D_{H^+}	$8.04 \cdot 10^{-5}$	$m^2 \cdot d^{-1}$	[b]
Diffusivity of biomass	D_X	$1 \cdot 10^{-7}$	$m^2 \cdot d^{-1}$	[c]
Biomass density	ρ	222	$mol \cdot m^{-3}$	[c]
Half saturation concentration of CO_2	K_{CO_2}	3.8	$mol \cdot m^{-3}$	[d]
Half saturation concentration of H_2	K_{H_2}	$8 \cdot 10^{-4}$	$mol \cdot m^{-3}$	[b]
Max growth rate of methanogens	$\mu_{X_{CH_4}}^{max}$	2.28	d^{-1}	[f]
Max growth rate of acetogens	$\mu_{X_{ac}}^{max}$	1.008	d^{-1}	[e]
Max growth rate of Hydrogenotrophs	$\mu_{X_{H_2}}^{max}$	2.2	d^{-1}	Assumed*1
Acetogenic growth yield	Y_{CH_4}	$6.8 \cdot 10^{-3}$	-	[f]
Methanogenic growth yield	Y_{ac}	$6 \cdot 10^{-3}$	-	[e]
Hydrogenotrophic growth yield	Y_{H_2}	$6.4 \cdot 10^{-3}$	-	Assumed
Boundary layer resistance	LL	$1 \cdot 10^{-4}$	M	[c]
Applied potential on cathode	E_{app}	Variant	V	[g]
Biofilm reactor volume	V	0.1	m^3	[c]
Cathodic biofilm surface area	A	10	m^2	[c]
Energy production of acetogenic cells	$f_{s,ac}^0$	0.067	-	Calculated*2 [h]
Energy production of methanogenic cells	f_{s,CH_4}^0	0.07	-	Calculated [h]
Stoichiometric coefficient of biomass in acetogenesis	-	0.0232	-	Calculated [h]
Stoichiometric coefficient of biomass in methanogenesis	-	0.028	-	Calculated [h]

[a] (Kazemi et al., 2015), [b] (Picioreanu et al., 2010), [c] (Reichert, 1998), [d] (Cabau-Peinado et al., 2021), [e] (Vandecasteele, 2016), [f] (Muñoz-Tamayo et al., 2019), [g] (Tremblay et al., 2019), [h] (Rittmann & McCarty, 2001).
*1. Different values are reported for hydrogenotrophic microbes. Here, the growth rate and yield are assumed based on hydrogenotrophic methanogens. (Berghuis et al., 2019; De Silva Muñoz et al., 2010) .
*2. The biomass formula is $C_5H_7O_2N$ (Metcalf et al., 2014).

Where, γ is the equal electron production, that for acetate and methane is 8, and for hydrogen is 2.

2.2. Simulation parameters, inputs, and outline

Simulation parameters are given in Table 1. The choice of cathodic voltage and relevant H^+ concentration was established from experimental work by Tremblay et al. where H_2 evolution depends on cathodic electric potential at ambient temperature 25° C (Tremblay et al., 2019). H^+ concentration from the experiment is scaled up to the reactor volume in the simulations. H^+ concentration depends highly on voltage, so at each step, H^+ concentration varies at the same time with voltage change at constant CO_2 concentration. The objective is to calculate the reduced CO_2 at each voltage and H^+ concentration. Also, picture the importance of H^+/H_2 concentration in CO_2 conversion efficiency. All varying steps is executed for both DIET and IMET mechanism to find the more efficient mechanism based on the defined model parameters and inputs. Furthermore, the effect of CO_2 concentration is simulated at three different levels at constant H^+ concertation and constant voltage to prove that controlling CO_2 concentration according to the available H^+ at the corresponding voltage is important to have the highest CO_2 reduction efficiency. Table 2 shows the simulation inputs.

Table 2. Substrate concentration and voltage inputs to the cathodic biofilm for each step.

Step	E_{app} (V vs SHE)	S_{H^+} ($mol \cdot m^{-3}$)	S_{CO_2} ($mol \cdot m^{-3}$)
1	-0.3	60	25
2	-0.4	70	25
3	-0.5	80	25
4	-0.6	120	25
5	-0.7	160	25
6	-0.7	160	10 ,25, 50

According to the inflow and the reactor volume, simulation is done at 1 day HRT for 400 days for step 1 to 5. For step 6, CO_2 concentration increases every 100 days for total 300 days.

Simulations include the change in state variables including concentration of acetate (S_{ac}), methane (S_{CH_4}), CO_2 (S_{CO_2}), H^+ (S_{H^+}), hydrogen (S_{H_2}) and biomass (hydrogen producing microbes (X_{H_2}), methanogens (X_{CH_4}) and acetogens (X_{ac})), current density (j), biofilm thickness (L_f), and the distribution of biomass through the biofilm in IMET and DIET mechanisms at different cathodic voltages and substrate concentration.

3. Results and discussion

3.1. Effect of voltage at constant CO_2 level

Figures 2 and 3 compare the simulated methane and acetate concentration in DIET and IMET models. In DIET (Figure 2), both acetate and methane are formed from day one. However, acetate concentration decreases over time at all hydrogen concentrations while methane production increases until day 300. Then acetate production reaches 0.02 $mol \cdot m^{-3} \cdot d^{-1}$ and methane production reaches steady state at 19.95 $mol \cdot m^{-3} \cdot d^{-1}$.

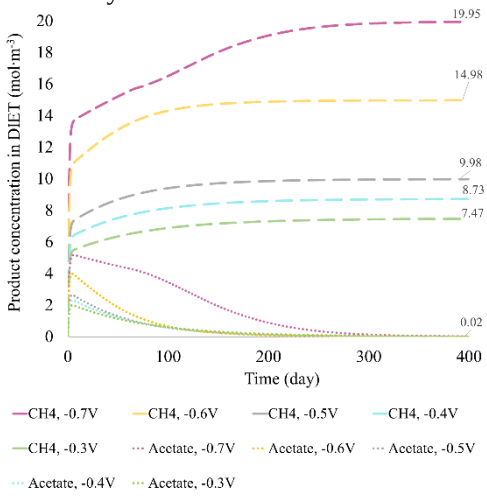

Figure 2. Acetate and methane concentration in DIET model at different potentials.

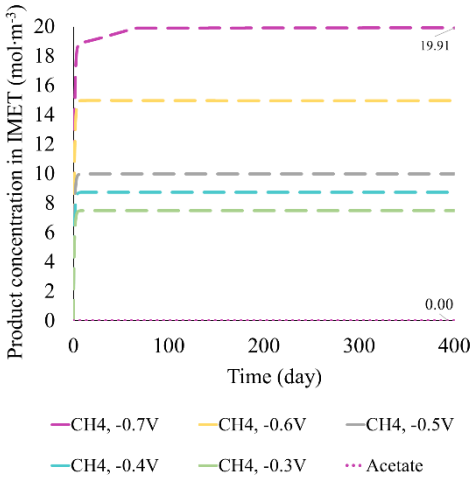

Figure 3: Acetate and methane concentration in IMET model at different potentials.

In IMET (Figure 3) acetogens fail to contribute to hydrogen uptake. Since the third species (hydrogenotrophs) contributes to the IMET model. In this case, diffusion of two CO_2 molecules toward acetogens for acetate formation will be limited. In IMET model, methane attains steady state in the first week at all voltages from -0.3 to -0.6 V. However, at -0.7 V, it takes 90 days for methane production to reach steady at 19.91 $mol \cdot m^{-3} \cdot d^{-1}$. Experimental studies also reported that methane production can be dominated by hydrogenotrophic methanogens via IMET (Gharbi et al., 2022).

However, in DIET model at steady state, the total amount of both products is 1.2% higher than in IMET model. Voltage increment has a positive impact on product formation in both mechanisms especially at -0.7 V which corresponds to higher concentration of H^+ ions, so more CO_2 can be reduced.

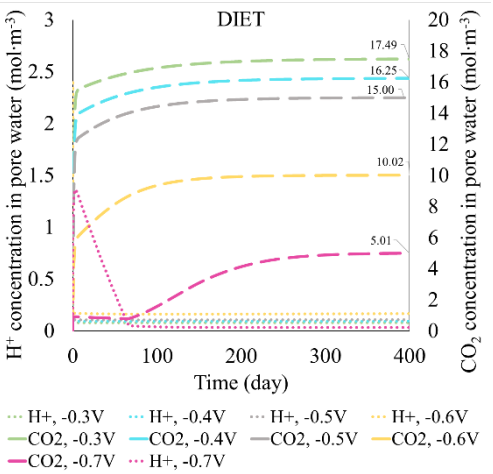

Figure 4. Unconsumed concentration of substrates in pore water in DIET model at different potentials.

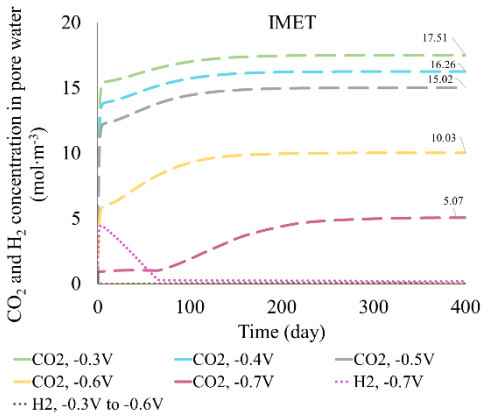

Figure 5: Unconsumed substrate concentration in pore water in IMET model at different potentials.

Figures 4 and 5 show the unconsumed substrate concentration in pore water. In DIET model (Figure 4), CO_2 consumption is slightly higher than IMET (80% for DIET and 79.7% for IMET). In both figures, higher voltage, which supplies more H^+ concentration, increases CO_2 consumption. Also, the highest unconsumed CO_2 in pore water refers to -0.3 V. All H^+ in DIET and all H_2 in IMET are consumed. This can give an idea of a real scenario that increasing CO_2 levels in an MES reactor without supplying enough H^+, cannot increase product formation. The simulation shows low CO_2 conversion efficiency at -0.3V in both mechanisms. The conversion increases gradually by increasing voltage to -0.7 V due to higher H^+ supply. However, at -0.7 V in the simulation, it takes longer for the system to stabilize the hydrogen consumption and CO_2 reduction.

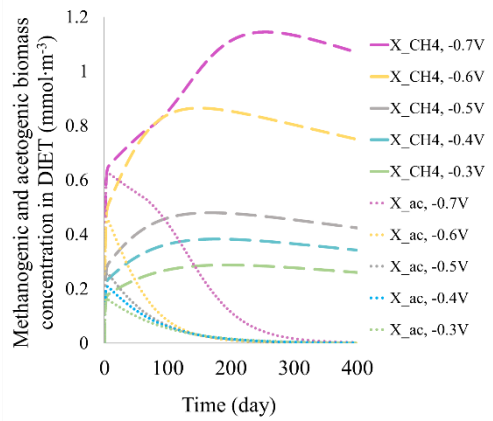

Figure 6. Electroactive biomass concentration in DIET model at different potentials.

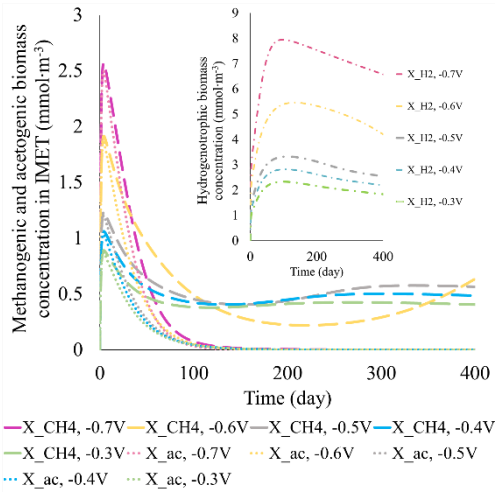

Figure 7. Biomass concentration in IMET model at different potentials.

Figures 6 and 7 show biomass concentration on the cathodic biofilm which in DIET model (Figure 6) consists of electroactive acetogens and methanogens. In IMET model (Figure 7) biomass concentration comprises acetogens, methanogens and electroactive hydrogenotrophs. In DIET, acetogenic and methanogenic biomass concentration change relatively. Finally, methanogens become dominant while acetogenic growth reaches close to zero. Methanogenic biomass attains maximum until day 300 then it follows a slow decreasing trend until day 400. That is due to the biofilm detachment velocity in the simulation. Increasing voltage in the simulation shows a positive effect on microbial growth and biomass concentration especially at -0.6 and -0.7 V. Figure 7 shows in IMET model, the dominant biomass is hydrogenotrophs with a concentration of 3.2 times higher than the total acetogenic and methanogenic biomass after 90 days. There is a

decline in acetogenic and methanogenic concentration while electroactive hydrogenotrophic biomass concentration reaches maximum 8 mmol·m^{-3} until day 90. Despite the electroactive biomass, acetogenic concentration attains zero at day 100, and methanogenic biomass concentration becomes stable between 0.5-1 mmol·m^{-3}. The decline in biomass may be according to microbial maintenance and detachment velocity parameters included in the simulated biofilm model.

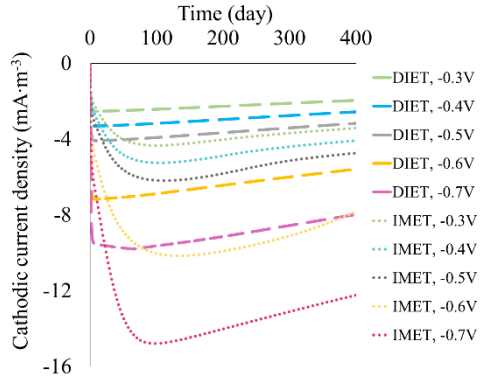

Figure 8. Generated current density in DIET and IMET models at different potentials.

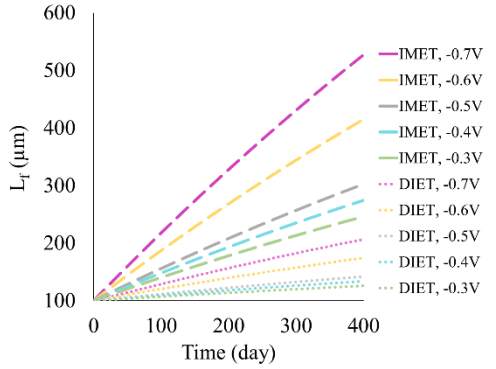

Figure 9. Biofilm thickness in DIET and IMET models at different potentials.

Figure 8 shows current density obtained from DIET and IMET models which is presented as $j\cdot(L_f)^{-1}$ in mA·m^{-3} related to electroactive biomass concentration. In DIET model, current density is calculated based on the total current consumed by electroactive acetogens and methanogens. In IMET, it is obtained according to electroactive hydrogenotrophs. In this simulation, the consumed current in DIET is lower than IMET (which corresponds to the total electron flow from anode to cathode). It rises by increasing voltage because of the growing biomass concentration. Considering -0.7 V at steady state, the current density is -7.8 in DIET and -12.22 mA·m^{-3} in IMET model. According to the simulations, DIET can fix 80% of CO_2 at 36% lower required current density. CO_2 conversion efficiency in the simulation with respect to energy consumption is higher in DIET model (regarding current density and consumed electrons). IMET model shows higher current density. The reason may be due to consuming more electrons and substrates for microbial growth and maintenance.

Figure 9 shows the simulated biofilm thickness. The five lower lines depict DIET, and the five upper lines correspond to IMET mechanisms. In the simulation, biofilm thickness increases by increasing the voltage due to higher biomass formation. However, L_f in DIET is 2.5 times thinner than IMET. Thinner biofilm in DIET at the same voltage can fix marginally higher CO_2 than IMET. In IMET, biofilm is 60% thicker than in DIET which is due to existence of hydrogenotrophs. According to the assumed parameters in the simulation, hydrogenotrophs can grow faster because they grow only on one substrate. So, they become the abundant biomass in IMET and increase the biofilm thickness.

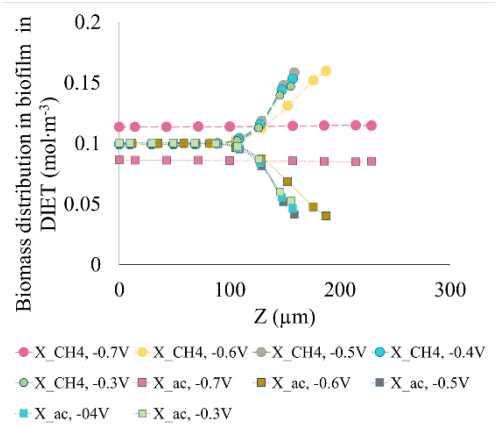

Figure 10. Acetogenic and methanogenic biomass distribution in biofilm in DIET model at different potentials.

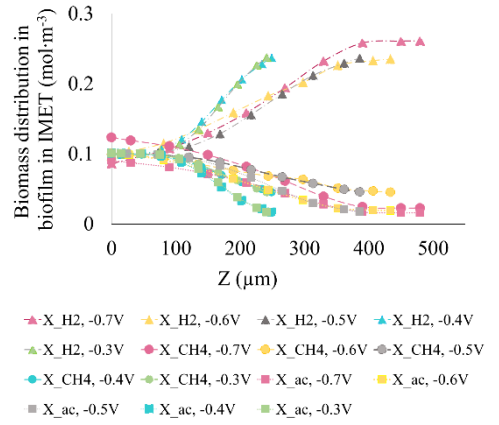

Figure 11. Hydrogenotrophic, acetogenic, and methanogenic biomass distribution through the biofilm in IMET model at different potentials.

Figures 10 and 11 show the simulated biomass distribution after 400 days in DIET and IMET. In

both models, biomass distribution has a direct relation with biofilm thickness. In DIET (Figure 10), distribution of both acetogens and methanogens is equal at the substratum (Z=0). The abundance of methanogens becomes higher in outer layers close to the pore water. In contrast, acetogenic community decrease at outer layers. That could be the reason for acetogenic decline in the simulation. The argument could be as the biofilm thickness is low at preliminary stages, acetate can be produced easier since the substrate diffusion is not limited by biofilm thickness. As the biofilm becomes thicker over time, methanogens will be dominant in outer layers which can uptake substrates from pore water faster than acetogens. Therefore, the dominant product is methane in the simulation after 400 days.

In the IMET model (Figure 11) most species in outer layers are hydrogenotrophs which consume all the H^+ to produce H_2. Compared to that, the abundance of acetogens and methanogens is almost equal at the substratum to the outer layers. However, acetogens grow by consuming two CO_2 molecules. If CO_2 reaches inner layers, methanogen which grow on one CO_2 molecule can consume it easier, so acetogens cannot produce acetate in such simulated conditions.

3.1. Effect of CO_2 concentration

Figures 12 and 13 resulted from run 6, indicate the effect of CO_2 concertation on product formation at a constant voltage of -0.7 V and constant H^+ concentration for both DIET and IMET mechanisms for 100 days each. In DIET model (Figure 12), the whole CO_2 (10 $mol \cdot m^{-3}$) is consumed in the presence of H^+. Following the stoichiometry of these biological reactions, 62% of H^+ remains unconsumed in pore water. If this happens in a reality, surplus H^+ may decrease the pH, or H^+ may be consumed in other possible reactions which are not desired. Increasing CO_2 concentration in the simulations, leads to full hydrogen consumption while CO_2 consumption efficiency reaches 80%. By further increase in CO_2 concentration, all the hydrogen will be consumed, while 60% of CO_2 remains unconsumed in pore water. If this is a case in real experiments, unused CO_2 may go out with methane due to gas/liquid CO_2 equilibrium and decrease the final methane concentration in biogas (Metcalf et al., 2014). The same trend can be seen in the simulated IMET (Figure 13) that at low CO_2 concentration, H_2 is not fully consumed. If such scenario happens, biogas may contain 82% H_2 and 18% CH_4 which is not desired. Reversely, at high CO_2 levels in the simulation, microorganisms consume all H_2, but in real cases, excess CO_2 may appear in biogas and decrease the biogas methane content according to biogas production theory (Metcalf et al., 2014).

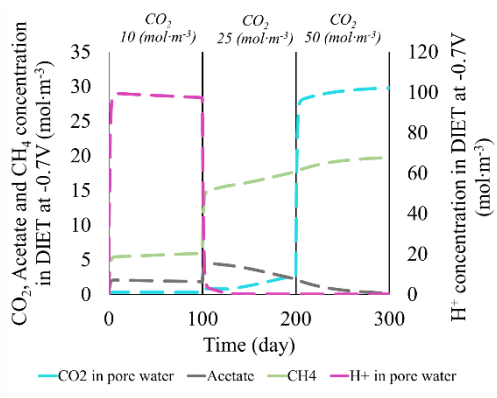

Figure 12. Effect of CO_2 concentration on acetate and CH_4 production in DIET model at -0.7V.

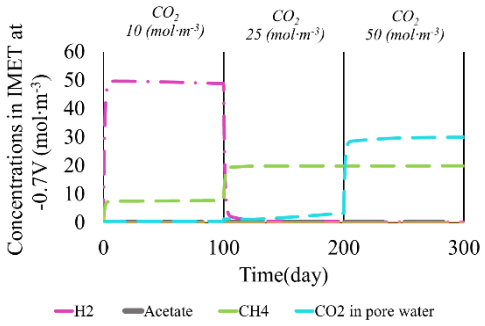

Figure 13. Effect of CO_2 concentration on acetate and CH_4 production in IMET model at -0.7 V.

4. Summary and conclusions

This work simulates CO_2 reduction to acetate and methane in a continuous flow MES reactor via IMET and DIET mechanisms at H^+ evolving potentials (-0.3 to -0.7 vs SHE) at constant CO_2 concentration, then at constant H^+ concentration and constant voltage. Simulation results show that higher voltage which could provide higher H^+ concentration could convert more CO_2 to methane and acetate in DIET model with 80% CO_2 fixation. Voltage increment could enhance product formation in both DIET and IMET models. Product formation in DIET model is calculated at 36% lower current density which shows it the more energy efficient mechanism compared to IMET model. Moreover, simulations show that controlling CO_2 concentration is another criterion of importance in limited source of H^+ supply.

DIET model implies to be more efficient than IMET model in CO_2 fixation. This means 1.2% higher product formation in DIET at steady state with 36% lower generated current. That means less energy requirement than in IMET mechanism. Not much particular work is available to compare DIET and IMET mechanisms in bioelectrochemical CO_2 fixation. The overall result of this simulation aligns with Stork et al. that DIET needs less energy in

form of electrons for CO_2 fixation. However, the simulations were done assuming simple conditions. Real MES reactors have complex microbial communities which may affect acetogenesis and methanogenesis. Also, intracellular, and extracellular limitations of diverse types of acetogens and methanogens, and their substrate uptake capacity is not studied in these simulations. The yield and maximum growth rate of the assumed microbes in the simulations are found in literature which might overestimate or underestimate the production in DIET or IMET models. Also, detachment velocity and diffusion phenomena are the only limitations included in the simulations. Moreover, there is a non-zero initial value for microbial concentration on the biofilm, so the product formation starts from the first day without a lag phase. However, in real reactors, the lag phase of microbial adaptation to start CO_2 fixation is longer (Metcalf et al., 2014). In these simulations, since H^+ is available from the first day, microbes start CO_2 reduction from the first day. This simulation studied the cathodic reactions for both mechanisms. However, electron generation source which depends on the available compounds for anode is an important measure of investigation at the next stage. The number of transferred electrons depends on the molecular compounds accessible to anodic biofilm for degradation at a certain voltage. Thus, the model can be completed by including anodic reactions.

References

Bajracharya, S., ter Heijne, A., Dominguez Benetton, X., Vanbroekhoven, K., Buisman, C. J. N., Strik, D. P. B. T. B., & Pant, D. (2015). Carbon dioxide reduction by mixed and pure cultures in microbial electrosynthesis using an assembly of graphite felt and stainless steel as a cathode. *Bioresource technology*, *195*, 14-24. https://doi.org/https://doi.org/10.1016/j.biortech.2015.05.081

Berghuis, B. A., Yu, F. B., Schulz, F., Blainey, P. C., Woyke, T., & Quake, S. R. (2019). Hydrogenotrophic methanogenesis in archaeal phylum Verstraetearchaeota reveals the shared ancestry of all methanogens. *Proceedings of the National Academy of Sciences*, *116*(11), 5037-5044. https://doi.org/doi:10.1073/pnas.1815631116

Cabau-Peinado, O., Straathof, A. J. J., & Jourdin, L. (2021). A General Model for Biofilm-Driven Microbial Electrosynthesis of Carboxylates From CO2 [Original Research]. *Frontiers in Microbiology*, *12*. https://doi.org/10.3389/fmicb.2021.669218

De Silva Muñoz, L., Bergel, A., Féron, D., & Basséguy, R. (2010). Hydrogen production by electrolysis of a phosphate solution on a stainless steel cathode. *International Journal of Hydrogen Energy*, *35*(16), 8561-8568. https://doi.org/https://doi.org/10.1016/j.ijhydene.2010.05.101

Flowers, P., & Theopold, K. (2019). *[eTextbook] Chemistry-2e*. OpenStax.

Gharbi, R., Vidales, A. G., Omanovic, S., & Tartakovsky, B. (2022). Mathematical model of a microbial electrosynthesis cell for the conversion of carbon dioxide into methane and acetate. *Journal of CO2 Utilization*, *59*, 101956.

Kazemi, M., Biria, D., & Rismani-Yazdi, H. (2015). Modelling bio-electrosynthesis in a reverse microbial fuel cell to produce acetate from CO 2 and H 2 O. *Physical Chemistry Chemical Physics*, *17*(19), 12561-12574.

Metcalf, Eddy, Abu-Orf, M., Bowden, G., Burton, F. L., Pfrang, W., Stensel, H. D., Tchobanoglous, G., Tsuchihashi, R., & AECOM. (2014). *Wastewater engineering: treatment and resource recovery*. McGraw Hill Education.

Muñoz-Tamayo, R., Popova, M., Tillier, M., Morgavi, D. P., Morel, J.-P., Fonty, G., & Morel-Desrosiers, N. (2019). Hydrogenotrophic methanogens of the mammalian gut: Functionally similar, thermodynamically different—A modelling approach. *PloS one*, *14*(12), e0226243.

Nelabhotla, A. B. T., & Dinamarca, C. (2018). Electrochemically mediated CO 2 reduction for bio-methane production: a review. *Reviews in Environmental Science and Bio/Technology*, *17*(3), 531-551.

Nelabhotla, A. B. T., & Dinamarca, C. (2019). Bioelectrochemical CO2 reduction to methane: MES integration in biogas production processes. *Applied Sciences*, *9*(6), 1056.

Nelabhotla, A. B. T., Pant, D., & Dinamarca, C. (2021). Power-to-gas for methanation. In *Emerging Technologies and Biological Systems for Biogas Upgrading* (pp. 187-221). Elsevier.

Picioreanu, C., van Loosdrecht, M. C. M., Curtis, T. P., & Scott, K. (2010). Model based evaluation of the effect of pH and electrode geometry on microbial fuel cell performance. *Bioelectrochemistry*, *78*(1), 8-24. https://doi.org/https://doi.org/10.1016/j.bioelechem.2009.04.009

Reichert, P. (1998). AQUASIM 2.0-Tutorial. *Swiss Federal Institute for Environmental Science and Technology (EAWAG): Dübendorf, Switzerland*.

Rittmann, B. E., & McCarty, P. L. (2001). *Environmental biotechnology: principles and applications*. McGraw-Hill Education.

Sivalingam, V., Dinamarca, C., Samarakoon, G., Winkler, D., & Bakke, R. (2020). Ammonium as a Carbon-Free Electron and Proton Source in Microbial Electrosynthesis Processes. *Sustainability*, *12*(8), 3081. https://www.mdpi.com/2071-1050/12/8/3081

Storck, T., Virdis, B., & Batstone, D. J. (2016). Modelling extracellular limitations for mediated versus direct interspecies electron transfer. *The ISME Journal*, *10*(3), 621-631. https://doi.org/10.1038/ismej.2015.139

Torres, C. I., Kato Marcus, A., & Rittmann, B. E. (2007). Kinetics of consumption of fermentation products by anode-respiring bacteria. *Applied microbiology and biotechnology*, *77*(3), 689-697.

Torres, C. I., Marcus, A. K., Parameswaran, P., & Rittmann, B. E. (2008). Kinetic Experiments for Evaluating the Nernst−Monod Model for Anode-Respiring Bacteria (ARB) in a Biofilm Anode. *Environmental Science & Technology*, *42*(17), 6593-6597. https://doi.org/10.1021/es800970w

Tremblay, P.-L., Faraghiparapari, N., & Zhang, T. (2019). Accelerated H2 Evolution during Microbial Electrosynthesis with Sporomusa ovata. *Catalysts*, *9*(2), 166. https://www.mdpi.com/2073-4344/9/2/166

Vandecasteele, J. (2016). Experimental and modelling study of pure-culture syngas fermentation for biofuels production. *MSc Universiteit Gent*, *356*.